

PAPER

A Real-Time Monitoring and Analysis Model for Regional Economic Activities Based on Mobile Computing

Chunmei Ren  

School of Information
Engineering, Xuzhou
University of Technology,
Xuzhou, China

rosabeibei@163.com**ABSTRACT**

With the rapid advancement of the digital economy, the dynamic and complex nature of regional economic activities has posed significant challenges to traditional low-frequency statistical monitoring methods. Mobile computing, with its capability to capture high-frequency and multi-source data, offers a promising new approach for real-time monitoring. However, current research still faces several limitations: low integration efficiency of heterogeneous data sources, insufficient fusion of spatiotemporal features, and significant interference from noise. Traditional statistical models, reliant on low-frequency sampled data, often suffer from lag and sampling bias. Although machine learning methods have improved predictive accuracy, models such as long short-term memory (LSTM) lack the ability to capture spatial heterogeneity; conventional denoising algorithms struggle to handle complex noise patterns; and many studies fail to fully explore the spatiotemporal coupling of economic activity. To address these issues, this study proposes a real-time monitoring and analysis model for regional economic activities based on mobile computing. The model consists of five core modules: (1) a data acquisition and preprocessing module for real-time integration and outlier detection across multiple data sources; (2) a denoising module based on the rime ice optimization (RIME) algorithm, which enhances robustness against noise through soft frost search and hard frost penetration mechanisms; (3) a spatial feature extraction module using graph attention networks (GAT) to model inter-regional economic relationships and capture spatial spillover effects; (4) a temporal feature extraction module based on LSTM to uncover long-term temporal dependencies; and (5) a prediction output module that fuses spatial and temporal features for accurate forecasting of economic activities. The innovation of this model lies in its optimized denoising process through the RIME algorithm and the deep integration of spatiotemporal features via GAT-LSTM. It supports real-time data input and dynamic prediction, providing an intelligent tool that transforms regional economic governance from “post-event analysis” to “real-time perception.” This contributes to more precise policymaking and more efficient resource allocation.

KEYWORDS

mobile computing, regional economic activities, real-time monitoring, rime ice optimization (RIME) algorithm, graph attention networks (GAT), long short-term memory (LSTM) model

Ren, C. (2025). A Real-Time Monitoring and Analysis Model for Regional Economic Activities Based on Mobile Computing. *International Journal of Interactive Mobile Technologies (IJIM)*, 19(18), pp. 49–62. <https://doi.org/10.3991/ijim.v19i18.58075>

Article submitted 2025-06-04. Revision uploaded 2025-07-28. Final acceptance 2025-08-05.

© 2025 by the authors of this article. Published under CC-BY.

1 INTRODUCTION

With the rapid development of the digital economy, the dynamics and complexity of regional economic activities [1–3] have significantly increased, and traditional monitoring methods based on sampling surveys and statistical reports [4–6] can no longer meet the demands for real-time and refined management. The widespread application of mobile computing technology [7–10] provides a new path to break through this bottleneck. High-frequency data collected through terminals such as smartphones and IoT devices [11, 12] can reflect the microscopic dynamics of regional economic activities in real time, providing a data basis for constructing dynamic monitoring systems. For example, traffic flow data has a correlation of over 60% with regional GDP, and consumption data generated by mobile devices [13, 14] can track commercial activity in real time. However, how to efficiently integrate multi-source heterogeneous data, accurately extract economic activity features, and achieve intelligent prediction remains a key challenge in current research.

Existing research methods have significant deficiencies when processing regional economic activity data. Traditional statistical models rely on low-frequency sampled data, which makes it difficult to capture instantaneous changes in economic activities, and suffer from data lag and sampling bias problems [15, 16]. Although machine learning methods have improved prediction accuracy, they face challenges of data noise interference and insufficient fusion of spatiotemporal features. For example, LSTM models [17] lack the characterization of spatial heterogeneity when processing time series data, and traditional denoising algorithms cannot effectively remove mixed noise in complex economic data. In addition, most existing studies focus on feature extraction from a single dimension and fail to fully explore the spatiotemporal coupling relationships of economic activities. For example, the model based on traditional statistical methods proposed in literature [18] has data lag problems, and the research in literature [19] shows that existing machine learning models have limitations in handling spatial heterogeneity.

To address the above problems, this paper proposes a real-time monitoring and analysis model for regional economic activities based on mobile computing. The model contains five core modules: (1) data acquisition and preprocessing module, which collects multi-source data in real time through mobile terminals and IoT devices, and performs format unification and outlier detection; (2) data denoising module based on the RIME algorithm, which effectively removes noise in data while preserving key information by using the algorithm's soft frost search strategy and hard frost penetration mechanism; (3) spatial feature extraction module based on GAT, which models economic associations between regions and captures spatial spillover effects and local agglomeration characteristics; (4) temporal feature extraction module based on LSTM, which mines long-term dependencies of economic activities through its gating mechanism; (5) prediction output module, which integrates spatiotemporal features to generate economic activity prediction results. The innovation of this model lies in three aspects: first, the data denoising process is optimized by the RIME algorithm, significantly improving the model's robustness to noisy data, especially suitable for high-frequency data processing scenarios in mobile computing; second, the combination of GAT and LSTM achieves deep fusion of spatiotemporal features of economic activities, enabling more accurate characterization of the dynamic evolution patterns of regional economy; finally, the model supports

real-time data input and prediction output, which can be applied in economic monitoring, policy evaluation, and other scenarios to provide intelligent tools for regional economic governance.

2 THE REAL-TIME MONITORING AND ANALYSIS MODEL OF REGIONAL ECONOMIC ACTIVITIES BASED ON MOBILE COMPUTING

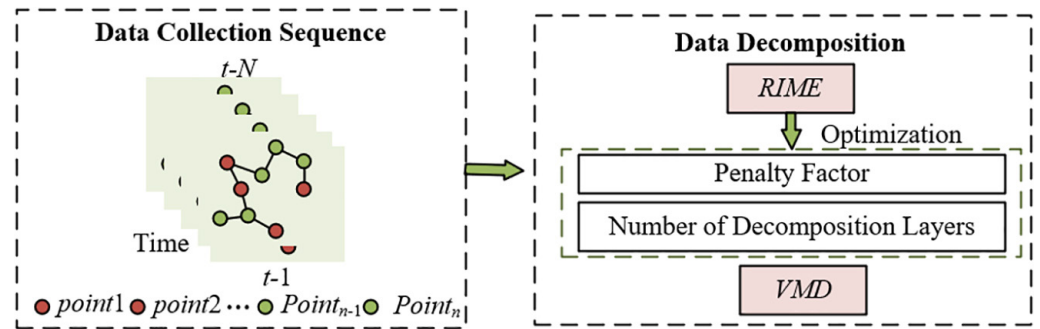


Fig. 1. Schematic diagram of data acquisition and preprocessing module

The model is constructed based on mobile computing technology, collecting multi-source heterogeneous data in real time through terminals such as smartphones and IoT devices, including location trajectories, consumption records, traffic flow, etc., forming high-frequency dynamic regional economic activity data sequences. Firstly, in the data acquisition and preprocessing module, the raw data are unified in format, outliers are filtered, and spatial gridding is performed to convert economic activity nodes in geographic space into graph-structured data. Regional units serve as nodes, and relationships such as population flow, logistics, and capital flow serve as edges, constructing a graph network that reflects regional economic connections and provides structured input for subsequent spatial feature extraction. Figure 1 presents a schematic diagram of the data acquisition and preprocessing module. To address the drawback of traditional variational mode decomposition (VMD) requiring manual parameter tuning, the model introduces the RIME algorithm to automatically optimize the decomposition level and penalty factor of VMD. Using envelope entropy minimization as the fitness function, through the iterative mechanisms of soft frost search and hard frost penetration, the optimal decomposition parameters are determined in one step, avoiding errors from manual intervention and achieving efficient denoising of noisy data. This lays a clean data foundation for spatiotemporal feature extraction. In the spatial feature extraction stage, the model improves upon the limitations of the traditional graph convolutional network (GCN) by employing GAT. Through the attention mechanism, neighbor nodes are assigned differentiated weights, accurately capturing asymmetric economic activity associations and local agglomeration effects among regions—for example, identifying the radiation driving effect of core regions on surrounding areas or the resource dependency of peripheral regions—thus compensating for GCN’s limitation of equal weighting when characterizing spatial dynamic correlations. Temporal feature extraction relies on the LSTM, which utilizes its gating mechanism to mine long-term dependencies in economic activity time series data, such as periodic fluctuations and trend changes. Figure 2 presents a schematic diagram of the spatiotemporal feature extraction in the model. Finally, through the prediction output module,

spatial spillover features extracted by GAT and temporal evolution patterns captured by LSTM are fused to construct a spatiotemporally coupled dynamic analysis model, realizing real-time monitoring and predictive forecasting of regional economic activities. This framework leverages the high-frequency data collection capability of mobile computing and the spatial modeling advantages of graph neural networks to form a full closed loop process of “data acquisition—noise optimization—spatiotemporal feature fusion—intelligent prediction.” It not only overcomes the low-frequency lag limitation of traditional methods but also enhances the model’s ability to analyze complex economic systems through automated parameter optimization and attention mechanisms, providing real-time and precise decision support for regional economic governance.

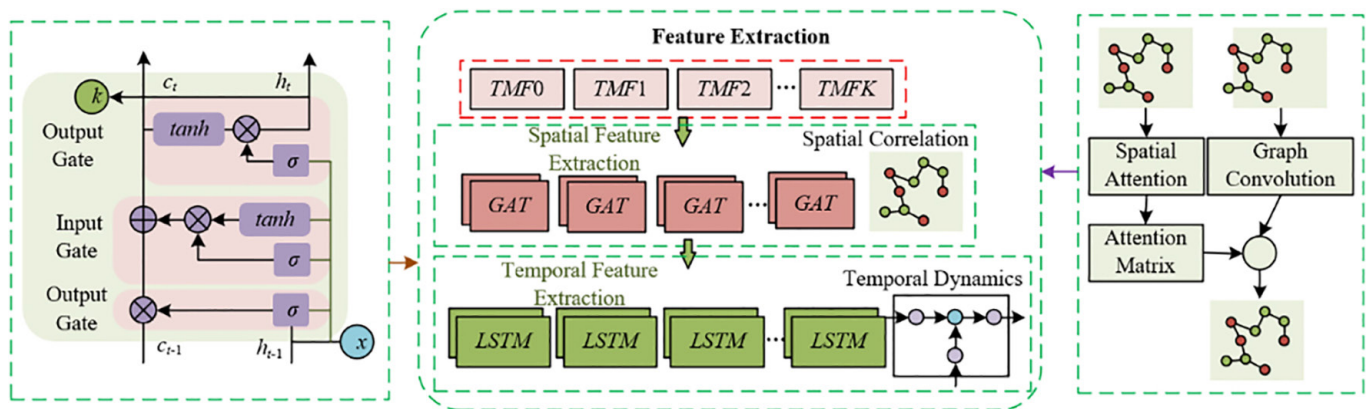


Fig. 2. Schematic diagram of spatiotemporal feature extraction in the model

2.1 RIME algorithm

The introduced rime algorithm consists of four stages:

Stage one: Fitness function definition and rime ice population initialization

The model first constructs a fitness function centered on envelope entropy, aiming to minimize the local envelope entropy of intrinsic mode functions (IMF) components obtained from VMD, thereby quantifying the degree of separation between noise and features in the data. Envelope entropy, as a sparsity indicator, effectively reflects the noise level in IMF components. When a component contains more noise, signal sparsity is weak, and envelopes entropy value is large; conversely, feature-dominant components exhibit strong sparsity and smaller entropy values. Based on this, the algorithm initializes a population composed of v rime ice agents, each agent containing f -dimensional rime ice particles corresponding to critical parameter combinations of VMD, forming an initial coverage of the parameter space to provide a search basis for subsequent optimization. Assuming the normalized form of $x(u)$ is represented by o_u , the envelope signal obtained by Hilbert demodulation of the signal $x(u)$ is represented by $x(u)$, the number of sampling points is V , the envelope entropy expression of signal $x(u)$ is:

$$\begin{cases} R_o = -\sum_{u=1}^V o_u \lg o_u \\ o_u = x(u) / \sum_{u=1}^V x(u) \end{cases} \tag{1}$$

Assuming the entire rime ice population is E , the population consists of v rime ice agents T_u , each agent composed of f rime ice particles a_{uk} . The ordinal number of the rime ice agent is denoted by u , and the ordinal number of the rime ice particle is denoted by k . The expressions are:

$$E = \begin{bmatrix} T_1 \\ T_2 \\ \vdots \\ T_u \end{bmatrix}; T_u = [a_{u1} a_{u2} \cdots a_{uk}] \tag{2}$$

$$E = \begin{bmatrix} a_{11} & a_{12} & \cdots & a_{1k} \\ a_{21} & a_{22} & \cdots & a_{2k} \\ \vdots & \vdots & \ddots & \vdots \\ a_{u1} & a_{u2} & \cdots & a_{uk} \end{bmatrix} \tag{3}$$

Stage two: Soft Frost search mechanism—global exploration under weak wind conditions

This stage simulates the random diffusion of rime ice particles in a weak wind environment to achieve global search in the parameter space. The particle position update formula introduces random variable e_1 and dynamic angle ϕ , enabling adaptive adjustment of the particle movement direction during the iteration process. Combined with the step function model of environmental factor β , it balances the randomness and directionality of the search. This mechanism covers the parameter space broadly, avoiding local optima, and is especially suitable for the complex noise characteristics of multi-source heterogeneous data in mobile computing scenarios, ensuring the algorithm can capture potential high-quality parameter combinations in the initial stage. Specifically, assuming the best rime ice agent's k -th particle in the population E is represented by E_{BE} , random number g is used to balance the center distance between two particles, and Iy_{uk} and My_{uk} represent the upper and lower bounds of the escape space, respectively, then the updated new position E_{uk}^{NE} of the rime ice particle under weak wind conditions is given by:

$$E_{uk}^{NE} = E_{BE} - j + e_1 \cdot \text{COS}\phi \cdot \alpha \cdot (g(Iy_{uk} - My_{uk}) + My_{uk}), e_2 < R \tag{4}$$

The mathematical expression of ϕ is given by:

$$\phi = \pi \cdot \frac{S}{10S} \tag{5}$$

In the soft frost search strategy, the parameter $[]$ represents rounding, and parameter μ is used to adjust the number of steps in the step function. The parameter α simulates the influence of the external environment, expressed as:

$$\alpha = 1 - \left[\frac{\mu \cdot S}{S} \right] / \mu \tag{6}$$

The attachment coefficient R and random number e_2 jointly control the update of the particle position. The mathematical expression of R is:

$$R = \sqrt{(s / S)} \tag{7}$$

Stage three: Hard frost penetration mechanism—local refinement under strong wind conditions

This stage simulates directional growth of particles under strong wind conditions, promoting information exchange between ordinary agents and the current best agent to improve parameter optimization accuracy. The algorithm guides particles to approach the position of the historical best solution, enhancing local search capability and conducting refined exploration in the neighborhood of the preliminarily locked high-quality parameters. This combination of “global exploration-local refinement” retains global space coverage ability while deepening the mining of optimal parameters, effectively solving the problem of incomplete noise removal caused by manual parameter tuning in VMD, and providing high-quality data with low noise interference for subsequent spatiotemporal feature extraction modules. Specifically, assuming the normalized fitness value of the current agent is represented by $D^{NO}(T_u)$, a random number e_3 in the range $(-1, 1)$, the replacement equation for particle position under strong wind conditions is given by:

$$E_{uk}^{NE} = E_{BE} - e_3 < D^{NO}(T_u) \quad (8)$$

Stage four: Forward greedy selection mechanism—iterative optimization and convergence determination

This stage uses a greedy strategy to compare the fitness values before and after particle updates. If the new solution’s envelope entropy is smaller, the parameter combination and fitness value of the current agent are replaced, ensuring the algorithm always iterates towards better solutions. This mechanism continuously filters high-quality solutions and gradually converges to the globally optimal parameter combination, which is finally applied to the VMD algorithm to realize adaptive decomposition of the original time series data. This process requires no manual intervention and relies on the high-frequency data processing capability of mobile computing to automatically achieve efficient separation of noise and features, laying a clean data foundation for subsequent spatiotemporal feature analysis based on graph neural networks, and significantly improving the model’s accuracy in analyzing the dynamic evolution of regional economic activities.

2.2 GAT

In monitoring regional economic activities, multi-source data collected by mobile computing are first converted into initial node feature vectors g_u , constructing a graph structure containing geographic spatial units, where nodes represent regional units and edges represent economic associations. To capture nonlinear feature relationships, a shared linear transformation Q is applied to each node, mapping original high-dimensional features to a low-dimensional space $Q\vec{g}$, achieving feature dimensionality reduction and spatial alignment. These operations not only reduce computational complexity but also provide a unified feature representation basis for the subsequent attention mechanism, suitable for fusion processing of multi-source heterogeneous data in mobile computing scenarios. For example, consumption data and traffic data at different scales can be mapped into the same feature space, facilitating the mining of implicit economic associations between regions. Specifically, assuming the importance of node k to node u is represented by r_{uk} , and any differentiable function is denoted by $\partial(\cdot)$, for all neighbor nodes k of the target node u :

$$r_{uk} = \partial(Q\vec{g}_u, Q\vec{g}_k) \quad (9)$$

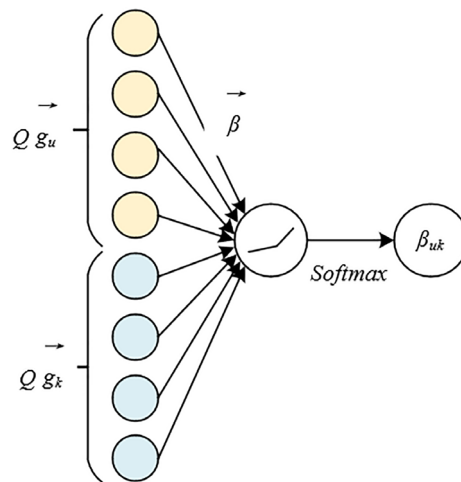


Fig. 3. Schematic diagram of node representation and update process under GAT

The attention coefficients r_{uk} between nodes are calculated through a single-layer feedforward neural network and the LeakyReLU activation function. This process explicitly models the feature interactions between the target node u and its neighbor nodes k , distinguishing the importance of different neighbors. For example, neighbor nodes of economic center regions receive higher attention weights. The negative slope property of LeakyReLU avoids the “dying neuron” problem, ensuring that weak connection features can still be effectively captured in sparse economic association scenarios, improving the model’s adaptability to unbalanced regional economic networks. Figure 3 shows the schematic diagram of node representation and update process under GAT. Assuming a v -dimensional column vector is represented by $Q\vec{g}$, the mathematical expression of r_{uk} is:

$$r_{uk} = \text{LeakyReLU}(\bar{x}^s(Q\vec{g}_u \parallel Q\vec{g}_k)) \tag{10}$$

To make attention weights comparable across nodes, the softmax function is used to normalize r_{uk} , resulting in the normalized weight β_{uk} , which reflects the contribution of neighbor node k to the feature update of target node u . In the feature aggregation stage, the normalized weights are multiplied by the corresponding transformed features of neighbor nodes and summed to generate the aggregated features of the target node. This process effectively fuses the spatial local correlation of regional economic activities, for example, by assigning neighbor weights to business district nodes to accurately capture the radiation effect of core business districts on surrounding retail outlets, providing structured feature support for real-time monitoring of commercial activity. Assuming the set of all neighbor nodes is represented by V_u , the mathematical expression of β_{uk} is:

$$\beta_{uk} = \text{SOFTMAX}(r_{uk}) = \frac{\exp(r_{uk})}{\sum_{j \in V_u} \exp(r_{uj})} \tag{11}$$

Multiplying β_{uk} by the corresponding neighbor node features $Q\vec{g}_k$, then summing and finally applying a softmax () function, generates the aggregated feature vector \vec{g}_u for each node:

$$\vec{g}_u = \delta\left(\sum_{k \in V_u} \beta_{uk} Q\vec{g}_k\right) \tag{12}$$

To address the sparsity problem of node features in complex graph structures, a multi-head attention mechanism executes multiple attention calculations in parallel, generating multiple differentiated weight matrices, which are finally integrated through concatenation or averaging into the final features. This mechanism iteratively updates node features multiple times, progressively strengthening the influence of key neighbors and suppressing noisy associations. For example, when identifying industrial clusters, multiple iterations more accurately capture the weight differences between upstream and downstream industry chain nodes. Through cyclic aggregation and update operations, the model can adapt to the dynamic evolution of regional economic networks, ensuring node features continuously converge with real-time data input and providing stable and spatially semantic-rich input data for subsequent temporal feature analysis combined with LSTM, ultimately achieving deep analysis of spatiotemporal coupling features of regional economic activities. Figure 4 shows the schematic diagram of node representation and update process under multi-head GAT. Assuming the output weights of each node are represented by \vec{g}_u^v , the number of adjacent nodes of node u is V_u , the attention mechanism weights after calculation are represented by β_{uk}^j , the nonlinear activation function is denoted by δ , and the number of iterations is v . The following formula gives the expression of node representation and update process under multi-head GAT when the number of iterations is 3:

$$\begin{aligned} \vec{g}_u^v &= \delta \left(\frac{1}{J} \sum_{j=1}^J \sum_{k \in V_u} \beta_{uk}^j Q^j \vec{g}_k' \right) \\ &\dots \\ \vec{g}_u^v &= \delta \left(\frac{1}{J} \sum_{j=1}^J \sum_{k \in V_u} \beta_{uk}^j Q^j \vec{g}_k'^{v-1} \right) \end{aligned} \tag{13}$$

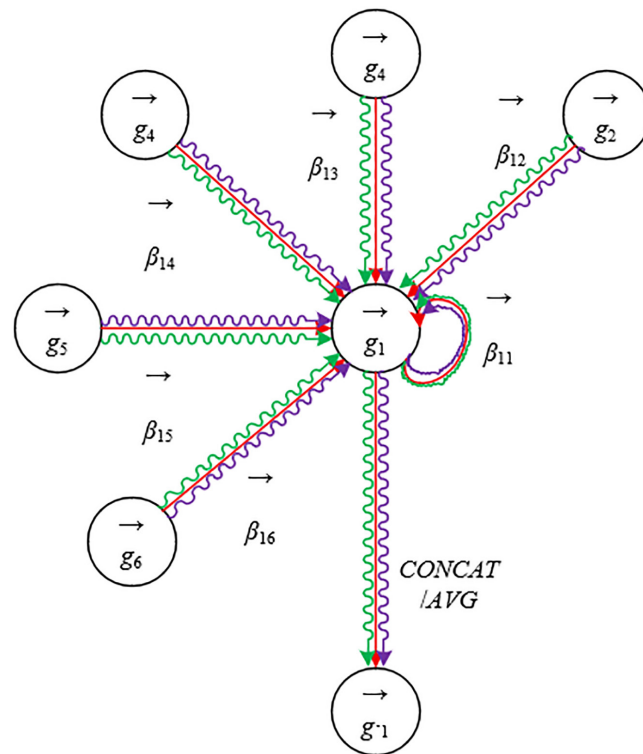


Fig. 4. Schematic diagram of node representation and update process under multi-head GAT

3 EXPERIMENTAL RESULTS AND ANALYSIS

From the comparison data of different optimization algorithms in Table 1, it can be seen that the RIME algorithm used in this paper shows significant advantages in the model's data denoising module. Compared with PSO and WOA, RIME has a VMD level of 6, a penalty factor of 1125, and a training time of only 1568, significantly improving the efficiency and accuracy of data preprocessing. This optimization result indicates that RIME, through the soft frost search and hard frost penetration mechanisms, can more efficiently and automatically optimize VMD parameters, effectively removing noise from multi-source economic data collected by mobile computing and providing clean, high-quality input data for subsequent spatial feature extraction based on GAT and temporal feature extraction based on LSTM networks.

From the comparison of overall model evaluation metrics in Table 2, it can be seen that after adopting the RIME algorithm, the proposed model significantly outperforms the PSO and WOA algorithms in prediction accuracy. Specifically, the RMSE (0.0826), MAE (0.0612), and MAPE (0.2235) corresponding to RIME are the smallest values. RMSE decreases by 6.77% compared to PSO and 3.28% compared to WOA; MAE decreases by 14.43% compared to PSO and 6.28% compared to WOA; MAPE decreases by 12.21% compared to PSO and 3.46% compared to WOA. This result indicates that the RIME algorithm, through the soft frost search and hard frost penetration mechanisms, efficiently optimizes VMD parameters and greatly improves data denoising effectiveness, laying a clean data foundation for subsequent spatiotemporal feature extraction. Experimental data intuitively demonstrate that the data denoising module optimized by RIME and the spatiotemporal feature fusion mechanism of GAT-LSTM jointly improve the model's prediction accuracy, enabling more accurate reflection of dynamic changes in regional economic activity monitoring. Compared with PSO and WOA, RIME's advantages in parameter optimization efficiency and noise handling precision directly translate into overall model performance improvement, validating the scientific nature of the "data acquisition-denoising optimization-spatiotemporal feature fusion-prediction output" architecture proposed in this paper.

Table 1. Comparison of optimization effects of different algorithms

Algorithm Name	VMD Level	Penalty Factor	Training Time
PSO	3	1896	2159
WOA	9	1136	2234
RIME	6	1125	1568

Table 2. Comparison of overall model evaluation metrics using different optimization algorithms

Algorithm Name	RMSE	MAE	MAPE
PSO	0.0886	0.0715	0.2546
WOA	0.0854	0.0653	0.2315
RIME	0.0826	0.0612	0.2235

From the comparison of model evaluation metrics over six iterations shown in Figure 5, it can be seen that as the number of iterations increases, the model's

prediction errors show a clear downward trend. Specifically, in the 1st iteration, MAPE is 0.8377, MAE is 0.1415, RMSE is 0.1757, indicating large errors that reflect insufficient noise removal and inadequate spatiotemporal feature fusion in the initial data; by the 6th iteration, MAPE decreases to 0.7025, MAE to 0.12, and RMSE to 0.1452, with significant error reduction. The 4th iteration yields the lowest error. This validates that the model proposed in this paper relies on the high-frequency data collection of mobile computing, optimizes data preprocessing through the RIME algorithm, and combines deep fusion of spatiotemporal features via GAT-LSTM, achieving high-precision real-time monitoring and analysis of regional economic activities through multiple iterative cycles. Compared with lower iteration counts, the model after multiple iterations shows qualitative improvements in noise processing, spatiotemporal feature characterization, and prediction accuracy, better reflecting the dynamic evolution of regional economic activities.

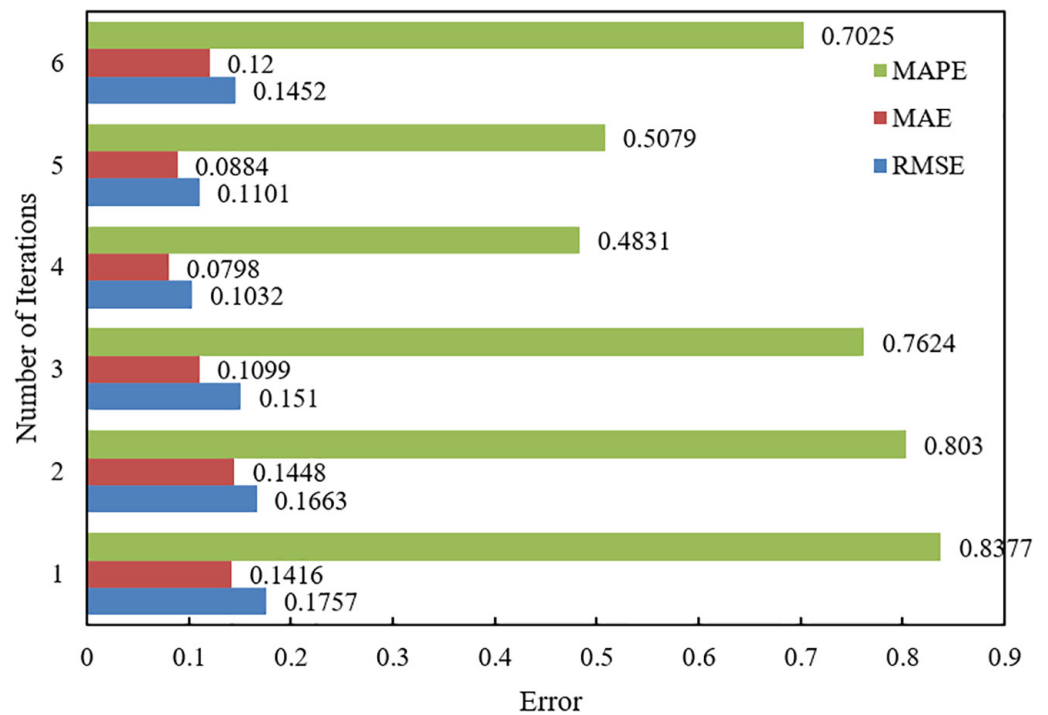


Fig. 5. Comparison of model evaluation metrics over 1 to 6 iterations

Table 3. Ablation study evaluation metrics of the model

Region	Model	RMSE	MAE	MAPE
1	Traditional GCN without VMD	0.5741	0.4325	2.7451
	Without VMD	0.5623	0.4123	2.7568
	Traditional VMD	0.1236	0.1125	0.6523
	Overall Model	0.1125	0.0785	0.4752
2	Traditional GCN without VMD	0.3785	0.2756	1.2356
	Without VMD	0.3652	0.2755	1.2586
	Traditional VMD	0.1325	0.0986	0.4452
	Overall Model	0.0985	0.0735	0.3256

(Continued)

Table 3. Ablation study evaluation metrics of the model (*Continued*)

Region	Model	RMSE	MAE	MAPE
3	Traditional GCN without VMD	0.3845	0.2651	1.1256
	Without VMD	0.3526	0.2542	1.1245
	Traditional VMD	0.0985	0.0723	0.3569
	Overall Model	0.0823	0.0612	0.2234

From the ablation study data in Table 3, it is evident that the overall model proposed in this paper significantly outperforms various ablation models in prediction error metrics across the three regions, fully validating its effectiveness. Taking region 1 as an example, the overall model's RMSE (0.1125), MAE (0.0785), and MAPE (0.4752) decrease by 80.4%, 82.0%, and 82.7% respectively, compared to the "Traditional GCN without VMD" model; decrease by 80.0%, 81.6%, and 82.4% compared to the "Without VMD" model; and decrease by 9.0%, 30.3%, and 27.2% compared to the "Traditional VMD" model. The comparison data of regions 2 and 3 show a consistent trend; for example, in region 2 the overall model RMSE is 0.0985, which is 74.0% lower than the "Traditional GCN without VMD" model, and in region 3 the RMSE is 0.0823, a 78.6% decrease. This result indicates that: first, the VMD denoising module based on the RIME algorithm efficiently removes noise from multi-source data collected by mobile computing through automatic parameter optimization, laying a clean data foundation for subsequent spatiotemporal feature extraction; second, the spatial feature extraction module based on GAT accurately models regional economic associations via the attention mechanism, enhancing the capture of spatial spillover effects and local agglomeration features; finally, the LSTM temporal feature extraction and spatiotemporal fusion prediction output module effectively mines the long-term dependencies of economic activities, and after deep fusion with GAT spatial features, achieves high-precision prediction of regional economic activities. Experimental data further validate the synergistic effect of the model's modules: RIME-optimized denoising ensures data quality, and GAT-LSTM fused spatiotemporal features enhance the model's generalization capability, both of which are indispensable.

From the fitting data comparison in Figure 6, it can be seen that the fit between the optimized model's prediction results and the real data is significantly higher than that before optimization, strongly proving the effectiveness of the model proposed in this paper. Regarding the fluctuation trend of the time series, the red curve before optimization shows obvious deviation from the real data, while the optimized curve almost coincides with the blue curve. Especially at the peaks and troughs in the time interval 20–30, the green curve accurately matches the real data values of 24.6 and 22.4, with minimal error. Experimental data show that the model achieves high-precision real-time monitoring and prediction of regional economic activities by combining RIME-optimized denoising and GAT-LSTM fused spatiotemporal features. The comparison of fitting before and after optimization intuitively demonstrates the model's significant advantages in noise processing and spatiotemporal feature capture: the red curve before optimization deviates from the real data by about 0.5–1.0 units, whereas the green curve after optimization shows almost no deviation, indicating that the model effectively solves the defects of traditional methods in noise interference and spatiotemporal feature separation and can more accurately reflect the real-time dynamics of regional economic activities.

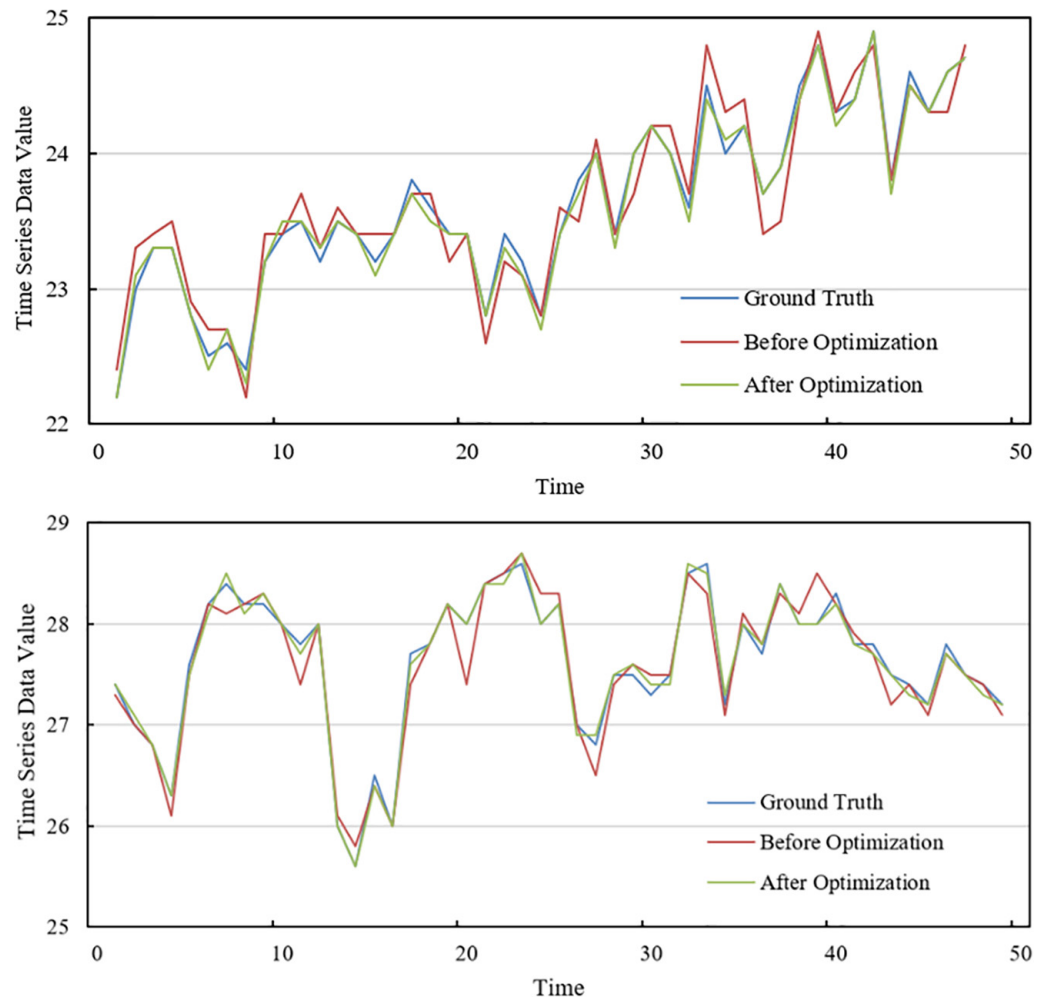


Fig. 6. Real-time monitoring and analysis data fitting of regional economic activities at different stages

4 CONCLUSION

This paper addressed the complexity and dynamics of real-time monitoring of regional economic activities in mobile computing scenarios, constructing an integrated five-module model including data acquisition and preprocessing, RIME-optimized denoising, GAT spatial feature extraction, LSTM temporal feature mining, and prediction output. The study solved the defects of traditional VMD manual parameter tuning through the soft frost search and hard frost penetration mechanisms of the RIME algorithm, automatically optimizing the decomposition levels and penalty factors by minimizing envelope entropy, significantly enhancing noise robustness of multi-source heterogeneous data; using GAT's attention mechanism to assign differentiated weights to regional nodes, accurately capturing spatial spillover effects and compensating for the equal weight defect of traditional GCN in modeling spatial dynamic correlations; combining LSTM's gating mechanism to mine long-term dependencies in time series, achieving deep fusion of economic activity spatiotemporal features and real-time prediction. Experimental results show the model performs significantly well in multi-regional economic activity monitoring, such as the high fit between optimized prediction curves and real data, validating the scientific nature of the full-process architecture “data acquisition—denoising optimization—spatiotemporal fusion—intelligent prediction,” providing

intelligent tools for regional economic governance from “post-event analysis” to “real-time perception,” and possessing important application value for improving policy accuracy and resource allocation efficiency.

Although this study achieves breakthroughs in noise handling and spatiotemporal feature fusion, its limitations mainly include: (1) dependence on mobile computing data may lead to insufficient data coverage in peripheral regions, affecting the model’s generalizability in economically underdeveloped areas; (2) the deep network structure of GAT-LSTM requires high computational resources, and real-time performance optimization still needs improvement; and (3) exogenous variables such as policy shocks and sudden events are not fully considered in their impact on economic activities. Future research can expand in the following directions: (1) introduce cross-modal data fusion technology to compensate for the limitations of single mobile data and enhance the model’s capability to analyze complex economic systems; (2) explore lightweight neural network architectures combined with edge computing technology to improve real-time monitoring efficiency; (3) incorporate causal inference mechanisms to quantify causal relationships between policy interventions and economic activities, promoting the model’s deep extension from “monitoring and analysis” to “decision support.” In addition, further validation of the model’s adaptability at different spatiotemporal scales can provide theoretical and methodological support for building multi-level, multi-dimensional regional economic monitoring systems.

5 REFERENCES

- [1] R. Pugh, E. Hamilton, S. Jack, and A. Gibbons, “A step into the unknown: Universities and the governance of regional economic development,” *European Planning Studies*, vol. 24, no. 7, pp. 1357–1373, 2016. <https://doi.org/10.1080/09654313.2016.1173201>
- [2] M. Beenstock, “Macroeconomics meets regional science: How national economic activity is related to regional economic activity,” *International Regional Science Review*, vol. 45, no. 3, pp. 321–351, 2022. <https://doi.org/10.1177/01600176211034140>
- [3] F. E. Malvicino, M. A. Pereira, and L. A. Trajtenberg, “Índices de actividad económica provincial en base a un modelo factorial dinámico. Argentina 1997–2019,” *Cuadernos del CIMBAGE*, vol. 22, no. 2, pp. 145–173, 2020.
- [4] N. V. Voroshilov, “Conceptual approach to the formation of the monitoring of socio-economic development of municipal entities in Russia’s regions,” *Economic and Social Changes: Facts, Trends, Forecast*, vol. 16, no. 3, pp. 118–140, 2023. <https://doi.org/10.15838/esc.2023.3.87.6>
- [5] Z. Brunarska, “Economic disengagement in state-society relations in Russia—Analysis of a household survey,” *Eurasian Geography and Economics*, vol. 56, no. 5, pp. 547–574, 2015. <https://doi.org/10.1080/15387216.2016.1151369>
- [6] T. Mousavi, S. Nikfar, and M. Abdollahi, “Comprehensive study on the administrative, economic, regional, and regulatory prospects of complementary and alternative medicine (CAM) in inflammatory bowel disease (IBD),” *Expert Review of Clinical Pharmacology*, vol. 14, no. 7, pp. 865–888, 2021. <https://doi.org/10.1080/17512433.2021.1925108>
- [7] T. Zhao, Z. Ma, X. Sun, Q. Yan, and D. Wang, “Dynamic prediction and optimization of energy consumption in mining equipment using mobile computing platforms,” *International Journal of Interactive Mobile Technologies (IJIM)*, vol. 19, no. 10, pp. 236–250, 2025. <https://doi.org/10.3991/ijim.v19i10.55837>
- [8] S. Manikanthan, T. Padmapriya, A. Hussain, and E. Thamizharasi, “Artificial intelligence techniques for enhancing smartphone application development on mobile computing,” *International Journal of Interactive Mobile Technologies (IJIM)*, vol. 14, no. 17, pp. 4–19, 2020. <https://doi.org/10.3991/ijim.v14i17.16569>

- [9] J. Lin, S. Huang, H. Zhang, X. Yang, and P. Zhao, “A deep-reinforcement-learning-based computation offloading with mobile vehicles in vehicular edge computing,” *IEEE Internet of Things Journal*, vol. 10, no. 17, pp. 15501–15514, 2023. <https://doi.org/10.1109/JIOT.2023.3264281>
- [10] K. Elgazzar, P. Martin, and H. S. Hassanein, “Cloud-assisted computation offloading to support mobile services,” *IEEE Transactions on Cloud Computing*, vol. 4, no. 3, pp. 279–292, 2014. <https://doi.org/10.1109/TCC.2014.2350471>
- [11] M. McGuire, K. N. Plataniotis, and A. N. Venetsanopoulos, “Estimating position of mobile terminals with survey data,” *EURASIP Journal on Advances in Signal Processing*, vol. 2002, p. 508712, 2002. <https://doi.org/10.1155/S1110865702000446>
- [12] T. Wada, S. Nakajima, and K. Ohtsuki, “Decision method of holding a mobile terminal and abnormal behavior by machine learning for ERESS,” *IEICE Communications Express*, vol. 10, no. 5, pp. 271–276, 2021. <https://doi.org/10.1587/comex.2021XBL0017>
- [13] K. Dutta and D. Vandermeer, “Caching to reduce mobile app energy consumption,” *ACM Transactions on the Web (TWEB)*, vol. 12, no. 1, pp. 1–30, 2017. <https://doi.org/10.1145/3125778>
- [14] H. Pihkola, M. Hongisto, O. Apilo, and M. Lasanen, “Evaluating the energy consumption of mobile data transfer—from technology development to consumer behaviour and life cycle thinking,” *Sustainability*, vol. 10, no. 7, p. 2494, 2018. <https://doi.org/10.3390/su10072494>
- [15] E. Iakovleva, E. Volkova, and T. Katermina, “Modeling of the system of regional indicators of the development of a circular economy,” *Nexo Scientific Journal*, vol. 36, no. 4, pp. 701–715, 2023. <https://doi.org/10.5377/nexo.v36i04.16796>
- [16] L. P. Georgescu, R. V. Ionescu, V. M. Antohi, M. L. Zlati, and C. Iticescu, “A new model for quantifying the impact of the social economy on the sustainability of water resources,” *Water*, vol. 17, no. 4, p. 561, 2025. <https://doi.org/10.3390/w17040561>
- [17] G. Xu, S. Peng, C. Li, and X. Chen, “Synergistic evolution of China’s green economy and digital economy based on LSTM-GM and grey absolute correlation,” *Sustainability*, vol. 15, no. 19, p. 14156, 2023. <https://doi.org/10.3390/su151914156>
- [18] D. Mügge and L. Linsi, “The national accounting paradox: How statistical norms corrode international economic data,” *European Journal of International Relations*, vol. 27, no. 2, pp. 403–427, 2021. <https://doi.org/10.1177/1354066120936339>
- [19] Y. Wang, C. Pan, X. Ni, C. Xue, J. Zhang, and J. Hu, “Investigation on the association between socio-economic multivariate data and fire incidence based on machine learning method: A case study in Shaanxi, China,” *Fire Technology*, vol. 61, pp. 1937–1968, 2024. <https://doi.org/10.1007/s10694-024-0167-w>

6 AUTHOR

Chunmei Ren, a Lecturer at the School of Information Engineering, Xuzhou University of Technology, holds a degree from China University of Mining and Technology. Her study focuses on computer vision, deep learning, image processing, and data analysis. She has published 15 academic papers, including three in Chinese core journals and one indexed by EI. She was the deputy editor-in-chief of two textbooks and owns 16 computer software copyrights. She led or contributed to five research projects (three provincials, one municipal, and one university-level) and 10 teaching reform projects (four municipal and six university-level). She guided students to win one first prize, one second prize, and four third prizes in provincial skill competitions (E-mail: rosabeibei@163.com).